Magnon-induced chaos in an optical $\mathcal{PT}$-symmetric resonator

Wen-Ling Xu, Xiao-Fei Liu, Yang Sun, Yong-Pan Gao, Tie-Jun Wang,* and Chuan Wang
School of Science and the State Key Laboratory of Information Photonics and Optical Communications, Beijing University of Posts and Telecommunications, Beijing 100876, China

(Received 30 June 2019; published 10 January 2020)

Optomagnonics supports optical modes with high-quality optical factors and strong photon-magnon interaction on the scale of micrometers. These novel features provide an effective way to modulate the electromagnetic field in optical microcavities. Here in this work, we studied the magnon-induced chaos in an optomagnonical cavity under the condition of parity-time symmetry, and the chaotic behaviors of electromagnetic field could be observed under ultralow thresholds. Even more, the existence optomagnetic interaction makes this chaotic phenomenon controllable through modulating the external field. This research will enrich the study of light matter interaction in the microcavity and provide a theoretical guidance for random number state generation and the realization of the chaotic encryption of information on chips.

DOI: 10.1103/PhysRevE.101.012205

I. INTRODUCTION

The achieving of strong interaction between photons and solid state is an important issue in the field of nanophotonics and quantum information science. On the micrometer scale, optical microcavities [1], including the silica microsphere and the silicon-based microresonators, localize the optical field with large intensity due to the high-quality factor and small mode volume which could enhance the Purcell factor [2,3] between the photons and the solid atoms. Along with the increment of the optical field in these microresonators, the nonlinear interaction between the mechanical (magnetic) field and the optical field is triggered, which are defined as the optomechanics and optomagnonics, respectively. These nonlinear effects are caused by the radiation pressure effect and the optomagnetic effect. During recent studies, optomechanics [4–12] and optomagnonics [13–16] have become two important approaches to realize the interaction between hybrid modes in optical microresonators. Usually, there is one mode in the electromagnetic degree of freedom and another mode in the mechanical or magnetic degree of freedom.

To be specific, in an optomagnonic resonator, both the magnons and photons are strongly localized in the resonator. This feature also ensures that there are strong interactions between magnons and photons in it. In addition, as magnons or spin waves are unique platforms for the realization of long-lifetime quantum memories [17,18] and quantum state transfer, the study of the optomagnonical cavity has attracted much attention. Recently, studies on the interaction between photons and magnons in optomagnonical cavity have explored, for example, the efficient magneto-optical coupling in whispering-gallery-mode (WGM) resonators [15,19–21]. Also, the pronounced nonreciprocity and asymmetry in the sideband signals have been observed [22]. In addition, the electromagnetic cavity-mediated phonon-magnon interaction has been investigated [23]. Moreover, the nonlinear dynamics such as the chaotic motions of cavity optomagnonics systems [24,25] have attracted more attention.

On the other hand, the photonic molecule [26] is an important concept in the coupled cavities system, which has been used since 1998 in electromagnetically interacting optical microcavities. The photonic molecule is constructed by a cluster of coupled optical microcavities. When individual optical microcavities are brought into close proximity, their optical modes interact and then form the photonic molecules, and their modes are usually called supermodes [27]. Several basic issues in quantum physics have been explored in the study of optical microresonators, for example, the parity-time ($\mathcal{PT}$) symmetry [28–31]. The concept of $\mathcal{PT}$ symmetry originated from the description of the properties of the Hamiltonian which has real eigenvalue even it contains an imaginary part. It was first mentioned theoretically in Ref. [28] and demonstrated experimentally in the higher-order harmonic oscillator scheme [32]. Recently, this concept has been extended to the research field of micro- or nano-optics [29,33–36]. $\mathcal{PT}$ symmetry can be practically used in various applications, such as in optical isolators [29] and high-resolution sensing [37]. Although people have done in-depth research on $\mathcal{PT}$-symmetry systems, studies on $\mathcal{PT}$-symmetric optomagnonical systems are still rare.

In this paper, we propose a $\mathcal{PT}$-symmetric optomagnonical system and investigate the chaotic behaviors of the field, which has been widely studied in various hybrid microcavity systems [38–40]. Yttrium iron garnet (YIG) spheres [41–44] are usually regarded as magnon resonators, but their potential as high-Q (as high as 3×10^6) optical WGM microresonators is always overlooked [15,45]. In our proposal, we excite the optical mode in the YIG sphere and first focus on the nonlinear characteristics of optical field affected by magnetic materials; when the intensity of the optical field approaches the chaotic threshold, the nonlinear system is accompanied by chaotic motion [46,47]. To analyze the chaotic behavior, the Lyapunov exponent [48] is numerically calculated and phase

*wangtiejun@bupt.edu.cn

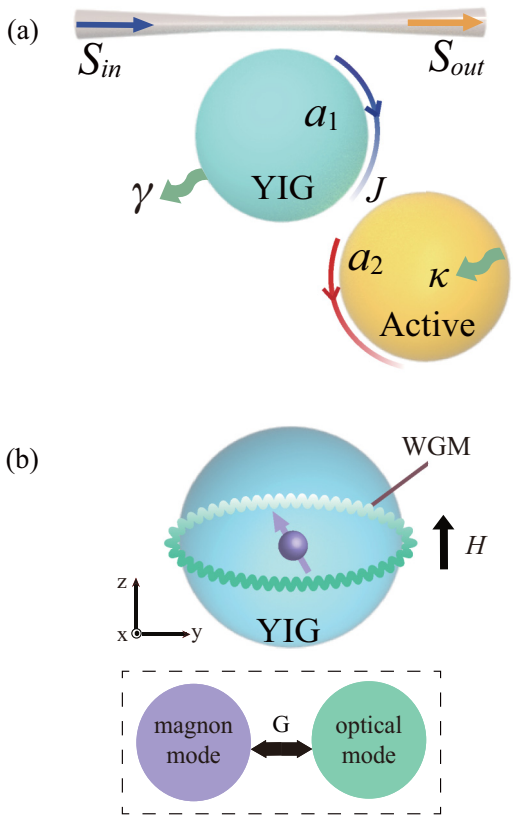

FIG. 1. Schematic diagram of an optomagnonical system. (a) WGM $\mathcal{PT}$-symmetric system including a YIG sphere a_1 coupled with an active cavity a_2 with coupling strength J. Here S_{in} and S_{out} represent input and output, respectively. The frequency and amplitude of the driving field are ω_d and Ω_d; γ represents the decay rate of optical mode in a_1 and κ represents the gain rate of cavity a_2. (b) Optomagnonic cavity with homogeneous magnetization along the z axis (an external magnetic field H is added along the z axis). The arrows represent the magnons with components in all directions. There is a localized optical mode with circular polarization in the y-z plane. The dotted line indicates the homogeneous magnon mode couples to the optical mode with strength G.

diagrams of the motion equation of photons are displayed. The nonlinear coefficient of photons is determined by the coupling strength and magnon, and thus the generation of chaos can be controlled by adjusting coupling strength or magnon. It is worth noting that magnon can be modulated by manipulating the external magnetic field [16], which provides us a reliable method for effectively controlling the chaotic behavior. Compared with normal coupled cavities, $\mathcal{PT}$-symmetric cavities have strong local field even under the circumstance of weak driving. Therefore, the generation of chaos only requires an ultralow threshold. Our research provides a method for generating random numbers and realizing secret information processing [49,50].

II. MODEL AND DYNAMICAL EQUATIONS

The $\mathcal{PT}$-symmetric optomagnonical system is shown in Fig. 1(a). The system shows a photonic molecule structure which consists of a YIG sphere coupled with an Er^{3+}/Yb^{3+}-doped microsphere [51] (there are also many other Er^{3+}/Yb^{3+}-doped microresonator [52,53] structures have been experimentally proven to be achievable). These two microspheres are coupled through an evanescent field with coupling strength J. The YIG sphere coupled to a fiber-taper is a passive cavity which supports a homogeneous Kittel magnon mode (i.e., the ferromagnetic resonance mode) [54] tuned at the resonant frequency $\Omega = 5$ MHz and an optical WGM. The Er^{3+}/Yb^{3+}-doped microsphere which supports an optical WGM is denoted as the active cavity. The magnetic polarons that exist in the YIG sphere are pumped by the external bias magnetic field [55]. The Hamiltonian of our system can be described as follows [39]:

$$\begin{aligned}\hat{H} &= \hat{H}_c + \hat{H}_m + \hat{H}_I \\ \hat{H}_c &= \hbar\Delta_c(\hat{a}_1^\dagger\hat{a}_1 + \hat{a}_2^\dagger\hat{a}_2) - \hbar J(\hat{a}_1^\dagger\hat{a}_2 + \hat{a}_1\hat{a}_2^\dagger) \\ &\quad + i\hbar\Omega_d(\hat{a}_1^\dagger - \hat{a}_1) \\ \hat{H}_m &= \hbar\Omega\hat{S}_z \\ \hat{H}_I &= -\hbar G\hat{S}_x\hat{a}_1^\dagger\hat{a}_1,\end{aligned} \tag{1}$$

where $\hat{a}_1^\dagger(\hat{a}_1)$ and $\hat{a}_2^\dagger(\hat{a}_2)$ are the creation (annihilation) operators for optical modes of the YIG sphere and the active cavity, respectively. These two modes have the same resonant frequency, denoted as ω_c. The passive cavity is driven by the field with frequency ω_d and amplitude Ω_d. G is the coupling strength of optomagnonic. Considering the system in a frame rotating with ω_d, the detuning of the frequency can be expressed as $\Delta_c = \omega_c - \omega_d$. In our proposed system, the YIG sphere is magnetized by an external bias magnetic field along z axis and can be used to control the precession with frequency Ω. In theory, Δ_c is the beat frequency formed by the interaction of the cavity and the input photon, and it resonates with magnons when $\Delta_c = \Omega$. In other words, under the action of the cavity, the pump light can resonate with the magnetons. Here we assume a magnetic system with spin $\mathbf{S} = (S_x, S_y, S_z)$ which is dimensionless. The coupling term between the magnon and optical mode in the YIG sphere is shown in $\hat{H}_I$. As shown in Fig. 1(b), we assume that the optical field couples only to the x component of the macrospin S with coupling coefficient G which is a constant depended by material [39] for convenience. Other parameters of this system are $(\gamma, \kappa, G, \Omega, S_x, \Delta_c, \Omega_d) = (1\text{ MHz}, 0.4\gamma, 5\times10^2\text{ Hz}, 5\text{ MHz}, 1\times10^6, \Omega, 1\times10^2\gamma)$ throughout this paper.

To explore the nonlinear dynamics of $\mathcal{PT}$-symmetric optomagnonical system, we focus on derivation of the coupled semiclassical Langevin equations of motion from Eq. (1) under the classical limit by considering the loss γ and gain κ of two cavities, respectively. The intrinsic spin Gilbert damping [56] of the YIG sphere is about 10^{-4} [43] which can be omitted in our scheme. In the case of mean-field approximation, the equations of motion can be expressed as follows:

$$\begin{aligned}\dot{S}_x &= -\Omega S_y \\ \dot{S}_y &= \Omega S_x + Ga_1^* a_1 S_z \\ \dot{S}_z &= -Ga_1^* a_1 S_y \\ \dot{a}_1 &= (-i\Delta_c - \gamma/2)a_1 + iJa_2 + iGS_x a_1 + \Omega_d \\ \dot{a}_2 &= (-i\Delta_c + \kappa/2)a_2 + iJa_1.\end{aligned} \tag{2}$$

Based on Eq. (2), the detuning eigenfrequencies can be obtained as $\Delta\omega = i(\kappa-\gamma)/4 + \sqrt{16J^2-(\kappa+\gamma)^2}/4$. Here $\Delta\omega$ is a complex number whose real part represents the frequency difference of the supermode and the imaginary part represents the linewidth. When J is enhanced to be comparable to the optical linewidth γ, the supermode appears around the center resonant frequency with splitting width $\Delta\omega = \sqrt{16J^2-(\kappa+\gamma)^2}/4$ due to the tunneling effect between loss and gain cavities. Equation (2) shows that the intracavity field and the magnon mode would effect each other during the evolution via the optomagnonical interaction. In our system, when $\Delta\omega = 0$, i.e., $J = (\gamma+\kappa)/4$, it approaches the exceptional point, where eigenvalues and corresponding eigenstates of the system coalesce. When $J > (\gamma+\kappa)/4$, the system exhibits $\mathcal{PT}$-symmetric characteristics, which will significantly affect the nonlinear dynamics. According to Eq. (2), the evolutionary trajectory of the system depends on the initial conditions. To describe this dependence, we introduce time-dependent perturbation $\vec{\delta} = (\delta S_x, \delta S_y, \delta S_z, \delta a_{1r}, \delta a_{1i}, \delta a_{2r}, \delta a_{2i})$, where δa_{jr} and δa_{ji} $(j = 1, 2)$ represent the real and imaginary parts of the corresponding perturbations, respectively. By ignoring the effects of high-order perturbations, we can obtain $\dot{\vec{\delta}} = \mathbf{M}\delta$ [57] with coefficient matrix $\mathbf{M}$ which is used to describe the divergence of nearby trajectories in the phase space. Each value in the matrix $\mathbf{M}$ can be regarded as an infinitesimally perturbation to the initial condition,

$$\mathbf{M} = \begin{bmatrix} 0 & -\Omega & 0 & 0 & 0 & 0 & 0 \\ \Omega & 0 & G\left(a_{1r}^2 + a_{1i}^2\right) & 2Ga_{1r}S_z & 2Ga_{1i}S_z & 0 & 0 \\ 0 & -G\left(a_{1r}^2 + a_{1i}^2\right) & 0 & -2Ga_{1r}S_y & -2Ga_{1i}S_y & 0 & 0 \\ -Ga_{1i} & 0 & 0 & -\gamma/2 & (\Delta_c - GS_x) & 0 & -J \\ Ga_{1r} & 0 & 0 & (-\Delta_c + GS_x) & -\gamma/2 & J & 0 \\ 0 & 0 & 0 & 0 & -J & \kappa/2 & \Delta_c \\ 0 & 0 & 0 & J & 0 & -\Delta_c & \kappa/2 \end{bmatrix}.$$

III. RESULT AND DISCUSSION

There is usually a chaotic region in nonlinear dynamical systems. One of the parameters that may affect the generation of chaos is the coupling strength J, which can be tuned by adjusting the distance of the two resonators. To study the influence of the coupling strength, we numerically solved Eq. (2) under different coupling intensities. We define $I_a = |a_1|^2$ as the optical intensity in cavity a_1 and the corresponding power spectrum $S(\omega)$ can be obtained by performing fast Fourier transform of I_a, i.e., $S(\omega) \propto |\int_{-\infty}^{+\infty} I_a e^{-i\omega t} dt|$, which can be directly measured [58]. Based on numerically results, the optical trajectories are presented in phase space, and the evolution of the optical intensity I_a and the logarithm of power spectrum $\mathrm{Ln}S(\omega)$ are illustrated in Fig. 2. For a fixed driving amplitude $\Omega_d = 1 \times 10^2\gamma$, the nonlinearity of intracavity field will be enhanced when the strength J is increased. We then turn to the time interval $8 \rightarrow 12$ μs where the system tends to stabilize. The system works in a state under the $\mathcal{PT}$ broken situation at weak coupling $J = 0.1\gamma$. The intensity of the optical field in cavity a_1 is small and the cavity mode can be periodically modulated. The trajectory in phase space is regular as shown in Fig. 2(a). On the other hand, when J is increased to 3γ, the system is at the state of $\mathcal{PT}$ symmetry, and the intensity of the optical field in YIG sphere is enhanced. The trajectory presents more complicated behavior in phase space and the power spectrum $\mathrm{Ln}S(\omega)$ is larger due to enormous energy accumulation. In addition, chaotic motions of the optical field become more obvious if we continue to increase the strength J to 8γ. The intensity of optical field in the cavity a_1 is so strong that the optical trajectories in phase space are much more complicated and the corresponding power distribution characterizes the emergence of chaotic motion.

To give quantitative description of the influence of J, the Lyapunov exponent with different J/γ is studied, as shown in Fig. 3. We define the parameter of perturbation $\delta I_a = |a_1 + \delta a_1|^2 - |a_1|^2$, whose logarithmic slope versus time t is regarded as the Lyapunov exponent [48]. When Lyapunov exponent is positive, it means that the disturbance is exponentially increasing and the system is sensitive to the initial conditions; in other words, it is approaching the chaotic region. Figure 3 presents that in the case of a given component of the macrospin $S_x = 1 \times 10^6$, the intensity of the electromagnetic field in cavity a_1 is enhanced as the increment of J/γ. It clearly shows that the chaotic motion appears when one tunes the coupling strength J so that the system is at the state of $\mathcal{PT}$ symmetry. It also should to be noticed that when $J/\gamma \sim 6$, the Lyapunov exponent is unstable. The reason is that the evolution of the system shows a certain randomness when the system is in a chaotic state. Therefore, even though the Lyapunov index is different, the chaotic properties of the system are still the same in this region. Moreover, in order to know if the chaos correspond to high or low intensity spin waves, we define a parameter $\eta = S_x/S$ to compare the value S_x with S, where S is the total spin expressed as $S = \sqrt{S_x^2 + S_y^2 + S_z^2}$. As shown in Fig. 4, because of the fluctuation phenomenon, one can observe that η exhibits periodical changing over time t (note that here we only give an example by $J = 8\gamma$ to illustrate the problem). Figure 4 indicates that the direction of the spin is resonant and it also proves that our waves are indeed spin waves. Then it is reasonable to use S_x to study the nature of spin waves.

As discussed earlier, as part of the $\mathcal{PT}$-symmetric optomagnonical system, the nature of the magnon in the system will inevitably affect the generation of chaos in the system. To study this influence, we investigate the variation of dynamical

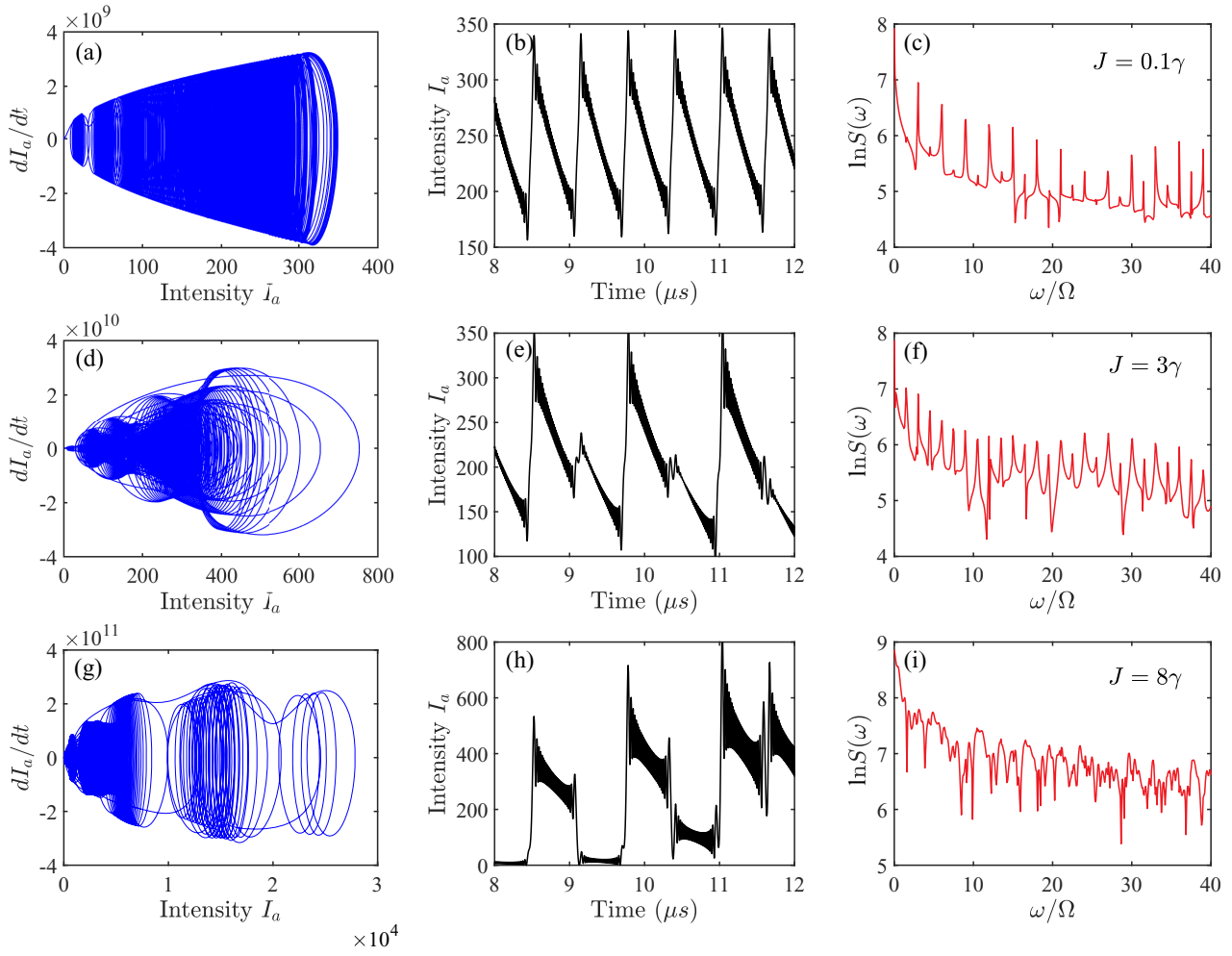

FIG. 2. Dependence of system dynamics on coupling strength J. Panels (a), (d), and (g) are optical trajectories in phase space; panels (b), (e), and (h) are the evolution of optical intensity I_a; and panels (c), (f), and (i) are corresponding power spectrum $\mathrm{Ln}S(\omega)$ changed over ω/Ω for different strength J. [(a)–(c)] $J = 0.1\gamma$. [(d)–(f)] $J = 3\gamma$. [(g), (h), and (i)] $J = 8\gamma$. The decay rate of YIG is $\gamma = 1$ MHz, the gain of active cavity is $\kappa = 0.4\gamma$, the coupling strength between magnon mode and optical mode is $G = 5 \times 10^2$ Hz, the precession frequency is $\Omega = 5$ MHz, the x component of the macrospin S is $S_x = 1 \times 10^6$, the detuning is $\Delta_c = \Omega$, and the driving amplitude is $\Omega_d = 1 \times 10^2\gamma$.

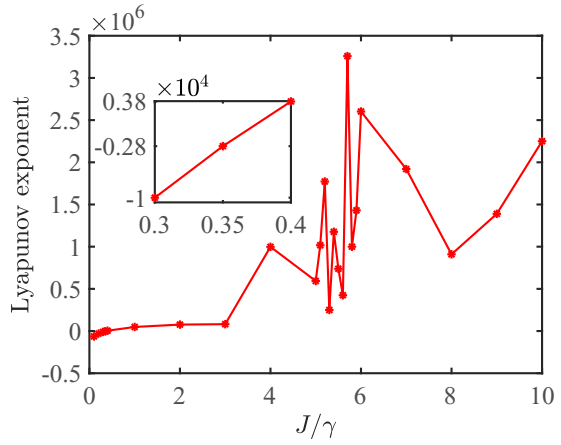

FIG. 3. Dependence of Lyapunov exponent on coupling strength J. Lyapunov exponent in cavity a_1 varies with different J/γ. The inset corresponds to the Lyapunov exponent for $J = 0.3\gamma$, $J = 0.35\gamma$, and $J = 0.4\gamma$. Other system parameters are the same as in Fig. 2.

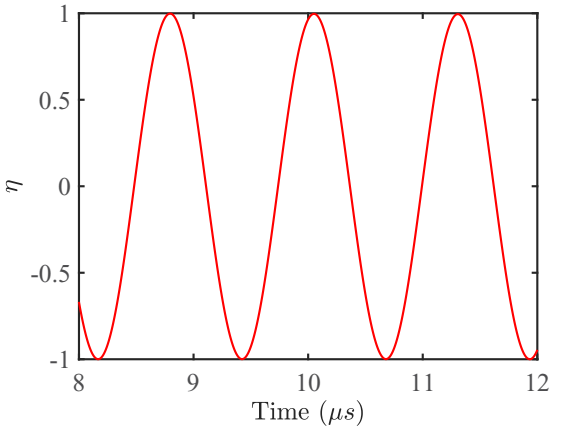

FIG. 4. Parameter η defined as S_x/S versus time t with $J = 8/\gamma$. Here S is the total spin with $S = \sqrt{S_x^2 + S_y^2 + S_z^2}$. Because of the fluctuation phenomenon, η exhibits periodical change over time t. Other system parameters are the same as in Fig. 2.

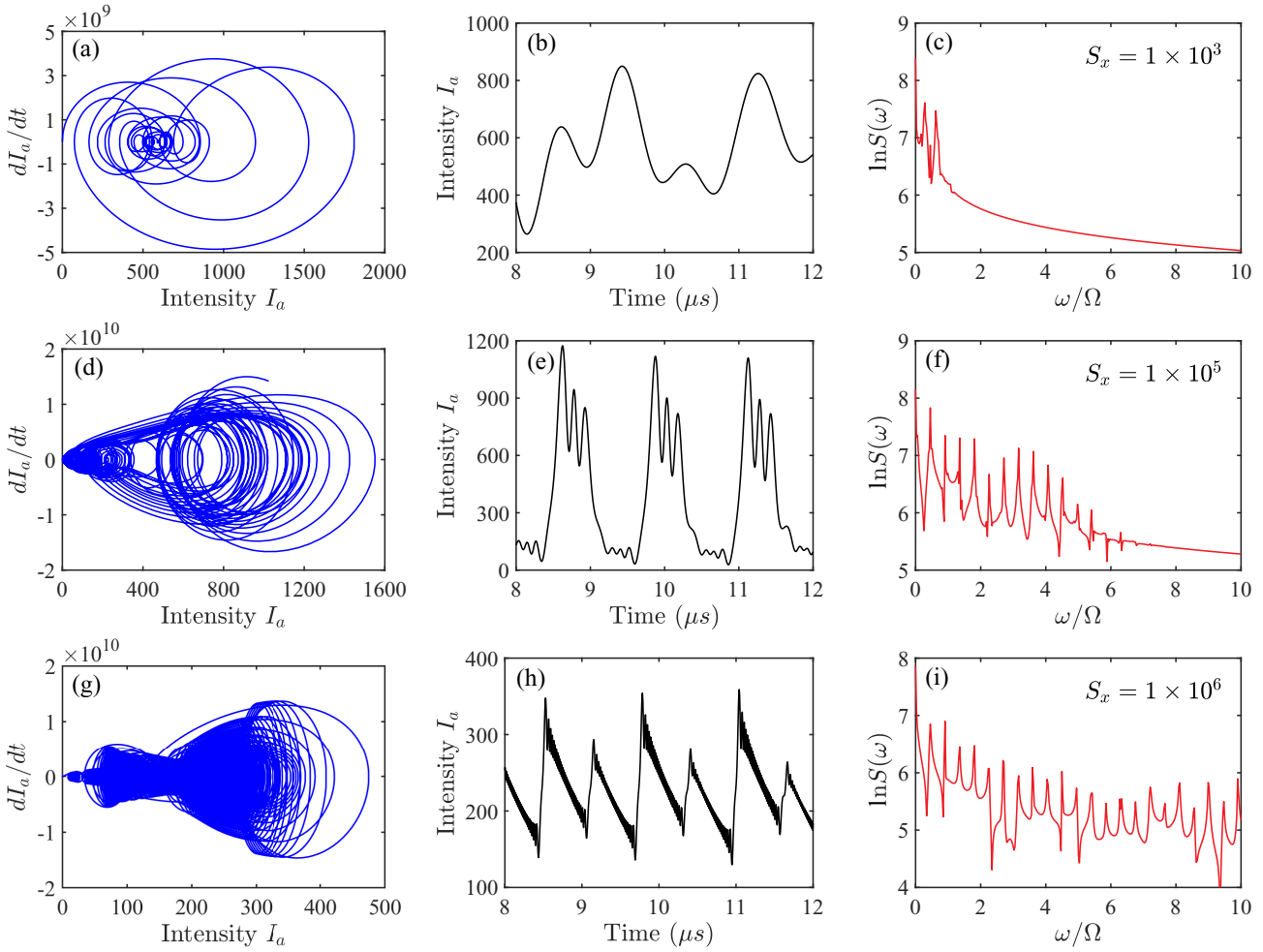

FIG. 5. Dependence of $\mathcal{PT}$-symmetric system dynamics on magnon. Panels (a), (d), and (g) are optical trajectories in the phase space; panels (b), (e), and (h) are the evolution of optical intensity I_a; panels (c), (f), and (i) are corresponding power spectrum $\mathrm{Ln}S(\omega)$ changed over ω/Ω for different S_x. (a) $S_x = 1 \times 10^3$. (b) $S_x = 1 \times 10^5$. (c) $S_x = 1 \times 10^6$. The coupling strength $J = 2\gamma$ between the two cavities is fixed, and other system parameters are the same as in Fig. 2.

behavior of system under different component of the magnon, as shown in Fig. 5. We present the dI_a/dt-I_a phase diagram in Figs. 5(a), 5(d) and 5(g); the time evolution of the optical intensity I_a in Figs. 5(b), 5(e) and 5(h); and the power spectrum in Figs. 5(c), 5(f) and 5(i). To ensure that the system works under the $\mathcal{PT}$-symmetric conditions, we set the coupling strength as $J = 2\gamma$. Then, by gradually increasing the strength of the magnon, the dynamics of our system could be observed. When the component is $S_x = 1 \times 10^3$ as shown in Figs. 5(a), 5(b) and 5(c), we can find the orbits in phase space show chaotic behavior, while there are only three main spectrums in the frequency domain. When the component S_x is increased to 1×10^5, the system is still chaotic, while amplitudes of sidebands have been greatly enhanced. It can be explained that the interactions between the photons and magnons are enhanced with the component of magnon increasing. Meanwhile, the optical nonlinearity of the system is strengthened because it is easier to exchange energy between photons and magnons under such strong interactions. Then the four-wave mixing process is more intensive, and the number of sidebands of the system gets larger. In order to verify our assumption, we increase S_x to 1×10^6, then the optical trajectories in the phase space are more complicated, and the chaotic phenomenon of the system is quite significant. On the other hand, the number of sidebands in the system continues increasing, which also confirms our previous assumption. Since the magnons can be controlled by an external bias magnetic field, the generation of the sidebands can be effectively controlled by the additional far field.

Previously, the effect of coupling strength is discussed based on whether the system is under $\mathcal{PT}$-symmetric conditions. It is still required to discuss the performance of the $\mathcal{PT}$-symmetric operation or the coupling strength on the chaos generation. To further classify the effects of $\mathcal{PT}$-symmetric operation and the coupling strength, the Lyapunov exponent is calculated in the passive-active (or $\mathcal{PT}$-symmetric) cavities coupled photonic molecule and passive-passive cavities coupled photonic molecule with different driving amplitude. We compare these two models in Fig. 6 under strong coupling $J = 3\gamma$. It is obvious that the driving threshold of chaos under the $\mathcal{PT}$-symmetric condition is much lower than the passive-passive coupled condition. The threshold value

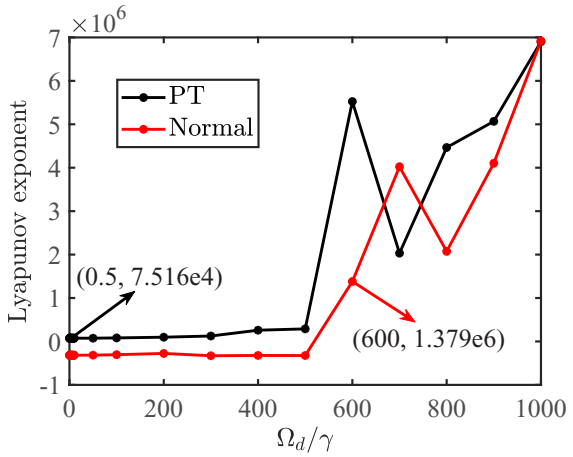

FIG. 6. Dependence of Lyapunov exponent on driving amplitude Ω_d. The red line indicates the effect of the driving amplitude on the Lyapunov exponent in the passive-passive system. When $\Omega_d = 6 \times 10^2\gamma$, Lyapunov exponent is positive and chaos will appear. The blue line indicates the effect of the driving amplitude on Lyapunov exponent in the $\mathcal{PT}$-symmetric system. When $\Omega_d = 0.5\gamma$, Lyapunov exponent is positive. System parameters are $\kappa = -0.4\gamma, J = 3\gamma$ and other parameters are the same as in Fig. 2.

$\Omega_d = 0.5\gamma$ of the $\mathcal{PT}$-symmetric condition is even lower than the dissipation of the cavity. Thus, we can conclude that the $\mathcal{PT}$ symmetry dominates the generation of chaos in our scheme. This conclusion also enriches the novelty of the $\mathcal{PT}$-symmetry system.

IV. DISCUSSION

The experimental value of the coupling strength between the magnon and photon is weak, but to our knowledge, there are several ways to enhance this interaction. First, the coupling strength G can be increased by the coupling the optical modes with the magnetic textures. If we can increase the mode volume of magnon or reduce the mode volume of the optical mode, then the coupling strength can obtain increased. It has been demonstrated in Ref. [59]. Second, the interaction can be effectively enhanced through pump-probe technology, which has been demonstrated experimentally [15]. Moreover, the coupling strength of our article can be reached by optimal mode matching, and it has been theoretically discussed in Ref. [60].

Moreover, because of the coupling between the electric field and the magnetization in Faraday-active materials, the electromagnetic energy is modified and expressed as [61]:

$$\hat{H}_{\mathrm{MO}} = -i\frac{\theta_F \lambda_n}{2\pi}\frac{\epsilon_0 \epsilon}{2}\int d\boldsymbol{rm}(\boldsymbol{r},t)\cdot[\boldsymbol{E}^*(\boldsymbol{r},t)\times\boldsymbol{E}(\boldsymbol{r},t)], \quad (3)$$

where $\boldsymbol{m}(\boldsymbol{r},t)$ is the magnetization in the sample. θ_F is the Faraday rotation per unit length λ_n and the prefactor $\frac{\theta_F\lambda_n}{2\pi} \sim 4 \times 10^{-5}$ in YIG. ϵ_0 and ϵ ($\sim$5 in YIG) are the vacuum and relative permittivity, respectively. Since $m(r,t)$ is related to the local spin operator which, in general, cannot be written as a linear combination of bosonic modes. In our proposal we consider the homogeneous Kittel mode where all spins precess in phase and can be replaced by a precessing macrospin, but, for example, in Ref. [59], the authors considered spin wave excitations on top of a possibly nonuniform static ground state $\boldsymbol{m}_0(\boldsymbol{r})$ and $\delta\boldsymbol{m}(\boldsymbol{r},t) = \boldsymbol{m}(\boldsymbol{r},t) - \boldsymbol{m}_0(\boldsymbol{r})$. In the case of $|\delta_m| \ll 1$, the harmonic oscillators corresponding to the magnon modes can be used to express these terms, and by quantizing the spin wave, they obtained the coupling Hamiltonian linearized in the spin fluctuations,

$$\hat{H}_{\mathrm{MO}} = \sum_{\alpha\beta\gamma} G_{\alpha\beta\gamma}\hat{a}_\alpha^\dagger\hat{a}_\beta\hat{b}_\gamma + \mathrm{H.c.}, \quad (4)$$

where $\hat{a}$ and $\hat{b}$ represent photon and magnon operators, respectively. $G_{\alpha\beta\gamma}$ is the optomagnonic coupling. This Hamiltonian is the same in form as our scheme but has a different physical meaning. Moreover, Eq. (4) is still nonlinear, since it contains interacting terms. Actually, as long as the system is nonlinear, the chaotic motion is expected. It can be demonstrated by our methods, for example, calculating the optical trajectories in the phase space and corresponding Lyapunov exponent. Moreover, according to our knowledge, if there is no nonlinearity in the system, then no chaos will occur in the system regardless of the form of magnetic excitations.

In summary, we have studied the chaotic behavior of the electromagnonic field in the optomagnetical photonic molecule under the $\mathcal{PT}$-symmetric condition and discussed the effective controlling method of the chaotic phenomenon. First, the effects of $\mathcal{PT}$ symmetry by adjusting the coupling strength between the passive and active cavities are presented. It is found that the electromagnetic field exhibits chaotic behavior even with weak optical drive. On the other hand, we also investigated influence of the strength of magnons in the passive optical microcavity. The result indicates that the strength of magnons is related to the four-wave mixing process, and then we can modulate the external bias magnetic field to control the generation of sidebands in the system. Even more, when the spin waves are strong enough, the sidebands of the system will become complicated, and the chaotic phenomenon of the system will be more obvious. Finally, we compared our scheme with passive-passive coupled cavities and found that the threshold of $\mathcal{PT}$-symmetric scheme is lower, which is conducive to the development of secret communications. The study proposes an achievable approach to control the nonlinear dynamics of the system, especially the generation of chaos, which paves the way for many important applications, such as the chaotic encryption of information and random numbers generation.

ACKNOWLEDGMENTS

The authors gratefully acknowledge the Project funded by the Ministry of Science and Technology of the People's Republic of China (2016YFA0301304), the National Natural Science Foundation of China through Grants No. 61622103 and No. 61671083, the Fok Ying-Tong Education Foundation for Young Teachers in the Higher Education Institutions of China (Grant No. 151063), the Fundamental Research Funds for the Central Universities.

[1] K. J. Vahala, Nature **424**, 839 (2003).
[2] E. M. Purcell, Phys. Rev. **69**, 37 (1946).
[3] S. Horoche and D. Kleppner, Phys. Today **42**, 24 (1989).
[4] M. Aspelmeyer, T. J. Kippenberg, and F. Marquardt, Rev. Mod. Phys. **86**, 1391 (2014).
[5] T. J. Kippenberg and K. J. Vahala, Science **321**, 1172 (2008).
[6] W. P. Bowen and G. J. Milburn, *Quantum Optomechanics* (CRC press, 2015).
[7] J. T. Hill, A. H. Safavi-Naeini, J. Chan, and O. Painter, Nat. Commun. **3**, 1196 (2012).
[8] B. Peng, Ş. K. Özdemir, W. Chen, F. Nori, and L. Yang, Nat. Commun. **5**, 5082 (2014).
[9] J. M. Torres, R. Betzholz, and M. Bienert, J. Phys. A: Math. Theor. **52**, 08LT02 (2019).
[10] S. Kolkowitz, A. C. B. Jayich, Q. P. Unterreithmeier, S. D. Bennett, P. Rabl, J. Harris, and M. D. Lukin, Science **335**, 1603 (2012).
[11] Y.-C. Liu, Y.-F. Xiao, X. Luan, and C. W. Wong, Phys. Rev. Lett. **110**, 153606 (2013).
[12] L.-L. Zheng, T.-S. Yin, Q. Bin, X.-Y. Lü, and Y. Wu, Phys. Rev. A **99**, 013804 (2019).
[13] X. Zhang, C.-L. Zou, L. Jiang, and H. X. Tang, Phys. Rev. Lett. **113**, 156401 (2014).
[14] T. Liu, X. Zhang, H. X. Tang, and M. E. Flatté, Phys. Rev. B **94**, 060405(R) (2016).
[15] X. Zhang, N. Zhu, C.-L. Zou, and H. X. Tang, Phys. Rev. Lett. **117**, 123605 (2016).
[16] A. Chumak, V. Vasyuchka, A. Serga, and B. Hillebrands, Nat. Phys. **11**, 453 (2015).
[17] V. Fiore, Y. Yang, M. C. Kuzyk, R. Barbour, L. Tian, and H. Wang, Phys. Rev. Lett. **107**, 133601 (2011).
[18] K. Stannigel, P. Komar, S. J. M. Habraken, S. D. Bennett, M. D. Lukin, P. Zoller, and P. Rabl, Phys. Rev. Lett. **109**, 013603 (2012).
[19] J. A. Haigh, S. Langenfeld, N. J. Lambert, J. J. Baumberg, A. J. Ramsay, A. Nunnenkamp, and A. J. Ferguson, Phys. Rev. A **92**, 063845 (2015).
[20] Y.-P. Wang, G.-Q. Zhang, D. Zhang, X.-Q. Luo, W. Xiong, S.-P. Wang, T.-F. Li, C.-M. Hu, and J. Q. You, Phys. Rev. B **94**, 224410 (2016).
[21] J. Bourhill, N. Kostylev, M. Goryachev, D. L. Creedon, and M. E. Tobar, Phys. Rev. B **93**, 144420 (2016).
[22] A. Osada, R. Hisatomi, A. Noguchi, Y. Tabuchi, R. Yamazaki, K. Usami, M. Sadgrove, R. Yalla, M. Nomura, and Y. Nakamura, Phys. Rev. Lett. **116**, 223601 (2016).
[23] Y.-P. Gao, C. Cao, T.-J. Wang, Y. Zhang, and C. Wang, Phys. Rev. A **96**, 023826 (2017).
[24] B. Wang, C. Kong, Z.-X. Liu, H. Xiong, and Y. Wu, Laser Phys. Lett. **16**, 045208 (2019).
[25] Z.-X. Liu, C. You, B. Wang, H. Xiong, and Y. Wu, Opt. Lett. **44**, 507 (2019).
[26] M. Bayer, T. Gutbrod, J. P. Reithmaier, A. Forchel, T. L. Reinecke, P. A. Knipp, A. A. Dremin, and V. D. Kulakovskii, Phys. Rev. Lett. **81**, 2582 (1998).
[27] Y. P. Rakovich, J. F. Donegan, M. Gerlach, A. L. Bradley, T. M. Connolly, J. J. Boland, N. Gaponik, and A. Rogach, Phys. Rev. A **70**, 051801(R) (2004).
[28] C. M. Bender and S. Boettcher, Phys. Rev. Lett. **80**, 5243 (1998).
[29] B. Peng, Ş. K. Özdemir, F. Lei, F. Monifi, M. Gianfreda, G. L. Long, S. Fan, F. Nori, C. M. Bender, and L. Yang, Nat. Phys. **10**, 394 (2014).
[30] R. El-Ganainy, K. G. Makris, M. Khajavikhan, Z. H. Musslimani, S. Rotter, and D. N. Christodoulides, Nat. Phys. **14**, 11 (2018).
[31] Q. Bin, X.-Y. Lü, T.-S. Yin, Y. Li, and Y. Wu, Phys. Rev. A **99**, 033809 (2019).
[32] A. Guo, G. J. Salamo, D. Duchesne, R. Morandotti, M. Volatier-Ravat, V. Aimez, G. A. Siviloglou, and D. N. Christodoulides, Phys. Rev. Lett. **103**, 093902 (2009).
[33] C. E. Rüter, K. G. Makris, R. El-Ganainy, D. N. Christodoulides, M. Segev, and D. Kip, Nat. Phys. **6**, 192 (2010).
[34] H. Jing, S. K. Özdemir, X.-Y. Lü, J. Zhang, L. Yang, and F. Nori, Phys. Rev. Lett. **113**, 053604 (2014).
[35] B. Wang, Z.-X. Liu, C. Kong, H. Xiong, and Y. Wu, Opt. Express **26**, 20248 (2018).
[36] B. Wang, Z.-X. Liu, C. Kong, H. Xiong, and Y. Wu, Opt. Express **27**, 8069 (2019).
[37] P.-Y. Chen, M. Sakhdari, M. Hajizadegan, Q. Cui, M. M.-C. Cheng, R. El-Ganainy, and A. Alù, Nat. Electron. **1**, 297 (2018).
[38] X.-Y. Lü, H. Jing, J.-Y. Ma, and Y. Wu, Phys. Rev. Lett. **114**, 253601 (2015).
[39] S. Viola Kusminskiy, H. X. Tang, and F. Marquardt, Phys. Rev. A **94**, 033821 (2016).
[40] H.-J. Chen, Q.-X. Ji, Q. Gong, X. Yi, and Y.-F. Xiao, *CLEO: Science and Innovations* (Optical Society of America, CA, US, 2019), pp. STh3J–2.
[41] W. Wettling, Appl. Phys. **6**, 367 (1975).
[42] D. D. Stancil, IEEE J. Quant. Electron. **27**, 61 (1991).
[43] D. D. Stancil and A. Prabhakar, *Spin Waves* (Springer, Berlin, 2009).
[44] D. L. Creedon, K. Benmessai, and M. E. Tobar, Phys. Rev. Lett. **109**, 143902 (2012).
[45] D. Wood and J. Remeika, J. Appl. Phys. **38**, 1038 (1967).
[46] T. Carmon, H. Rokhsari, L. Yang, T. J. Kippenberg, and K. J. Vahala, Phys. Rev. Lett. **94**, 223902 (2005).
[47] F. Monifi, J. Zhang, Ş. K. Özdemir, B. Peng, Y.-x. Liu, F. Bo, F. Nori, and L. Yang, Nat. Photon. **10**, 399 (2016).
[48] V. I. Oseledec, Trans. Moscow Math. Soc. **19**, 197 (1968).
[49] A. Argyris, D. Syvridis, L. Larger, V. Annovazzi-Lodi, P. Colet, I. Fischer, J. Garcia-Ojalvo, C. R. Mirasso, L. Pesquera, and K. A. Shore, Nature **438**, 343 (2005).
[50] M. Sciamanna and K. A. Shore, Nat. Photon. **9**, 151 (2015).
[51] Y. Huang, Y. Huang, P. Zhang, and C. Guo, AIP Adv. **4**, 027113 (2014).
[52] L. He, Ş. K. Özdemir, J. Zhu, W. Kim, and L. Yang, Nat. Nanotechnol. **6**, 428 (2011).
[53] X.-F. Liu, F. Lei, M. Gao, X. Yang, C. Wang, Ş. K. Özdemir, L. Yang, and G.-L. Long, Opt. Express **24**, 9550 (2016).
[54] C. Kittel, Phys. Rev. **73**, 155 (1948).
[55] Y.-P. Wang, G.-Q. Zhang, D. Zhang, T.-F. Li, C.-M. Hu, and J. Q. You, Phys. Rev. Lett. **120**, 057202 (2018).
[56] T. L. Gilbert, IEEE Trans. Magn. **40**, 3443 (2004).

[57] T. Carmon, M. C. Cross, and K. J. Vahala, Phys. Rev. Lett. **98**, 167203 (2007).
[58] G. Bergland, IEEE Spectrum **6**, 41 (1969).
[59] J. Graf, H. Pfeifer, F. Marquardt, and S. Viola Kusminskiy, Phys. Rev. B **98**, 241406(R) (2018).
[60] S. Sharma, B. Z. Rameshti, Y. M. Blanter, and G. E. W. Bauer, Phys. Rev. B **99**, 214423 (2019).
[61] L. Landau and E. Lifshitz, *Course of Theoretical Physics* (Elsevier, Amsterdam 2013).